RSC Advances

PAPER

View Article Online
View Journal | View Issue

Cite this: *RSC Adv.*, 2020, **10**, 8558

Effects of the novel catalyst Ni–$S_2O_8^{2-}$–K_2O/TiO_2 on efficient lignin depolymerization†

Jindong Wang,[a] Wenzhi Li, *[a] Huizhen Wang,[a] Ajibola Temitope Ogunbiyi,[a] Xiaomeng Dou[a] and Qiaozhi Ma[b]

To improve the utilization of lignin, much effort has been devoted to lignin depolymerization with the aim to decrease waste and enhance profitability. Here, a dual property (acid and base) catalyst, namely $S_2O_8^{2-}$–K_2O/TiO_2, was carefully researched. Upon loading $S_2O_8^{2-}$ and K_2O onto TiO_2, acid and base sites emerged, and $S_2O_8^{2-}$ and K_2O mutually enhanced the acid and base strengths of the catalyst enormously; this indeed facilitated lignin depolymerization. Under appropriate conditions, the yields of liquid product, petroleum ether soluble (PE-soluble) product and total monomer products were 83.76%, 50.4% and 28.96%, respectively. The constituents of the PE-soluble fraction, which are mainly monomers and dimers, can be used as liquid fuels or additives. In addition, after the catalyst was modified by Ni, better results were obtained. Surprisingly, it was found that the Ni enhanced not only the hydrogenation capacity but also the acidity. The highest high heating value (HHV) of the liquid product (33.6 MJ kg^{-1}) was obtained, and the yield of PE-soluble product increased from 50.4 to 56.4%. The product can be utilized as a fuel additive or be converted to bio-fuel. This catalysis system has significant potential in the conversion of lignin to bio-fuel.

Received 18th December 2019
Accepted 12th February 2020

DOI: 10.1039/c9ra10675h

rsc.li/rsc-advances

1. Introduction

Increasing awareness of global environmental protection and the finiteness of petroleum-based fuels are among key reasons for seeking a series of promising alternatives to traditional fossil fuels. Biomass, the only carbon-neutral energy source, is renowned as a promising source of synthetic liquid fuels and fine chemicals.[1] However, the scale of the biomass industry is not as large as it should be for many reasons. In China, for example, the lack of proper handling methods of the abundant agricultural crop residues causes many problems; therefore, finding efficient handling methods has drawn much attention.[2,3] Lignocellulosic biomass contains cellulose, hemicellulose and lignin.[4] Cellulose and hemicelluloses can be easily converted into fuels or other useful products.[5–9] However, the complex, three-dimensional, amorphous polymeric structure of lignin[10] prevents its wide usage in industrial fine chemical production. In fact, little lignin, a byproduct of the paper industry, is efficiently utilized.[11] Therefore, the lignin research community is unrelenting in its quest to find efficient methods of lignin depolymerization. Depolymerization is an important method for utilizing lignin well as it can convert lignin into aromatic monomers,[12,13] which can serve as valuable precursors to obtain further biopolymers or additives for biofuels.[14,15]

The major thermochemical routes for catalytic lignin transformation are pyrolysis, solvolysis, and hydrothermal catalytic processes.[16,17] Pyrolysis takes place at high temperatures (over 500 °C), usually with zeolite catalysts, to obtain liquid fuels and aromatics.[18–20] However, high temperature affords low-value char (20 to 40 wt%) and low yields of aromatics.[21] Lignin solvolysis generates a wide range of monomer products; however, their yields cannot be compared with those obtained by other methods.[23] Hydrothermal catalytic processes for lignin depolymerization have many advantages, such as moderate reaction conditions, high depolymerization efficiency and high conversion rate.[22,23] Hence, such a process was considered in this work. According to the phase of a catalyst, the catalytic process can be simply divided into two categories, namely homogeneous and heterogeneous catalysis.[23] Homogeneous catalysts generally afford higher production yields; however, due to the difficulty of separation, they are less desirable.[24–26] Because heterogeneous catalysts can be more easily recycled in most conditions, researchers have paid more attention to heterogeneous catalytic depolymerization of lignin.[27] The heterogeneous catalytic process mainly includes acid catalysis, base catalysis, hydroprocessing and oxidation.[22] Past studies have mostly focused on the use of mono-functional catalysts in depolymerization processes. For example, X. Zhang reported a method of hydrodeoxygenation of lignin-derived phenolic

[a]*Laboratory of Basic Research in Biomass Conversion and Utilization, Department of Thermal Science and Energy Engineering, University of Science and Technology of China, Hefei 230026, PR China. E-mail: liwenzhi@ustc.edu.cn*

[b]*College of Materials and Energy, South China Agricultural University, Guangzhou 510000, PR China*

† Electronic supplementary information (ESI) available. See DOI: 10.1039/c9ra10675h

compounds over Ni/SiO_2–ZrO_2 catalysts.[28] M. Grilc and B. Likozar employed a series of Ni–Mo catalysts for lignin hydrodeoxygenation.[29,30] Y. Ye used Ru/C to selectively produce 4-ethylphenolics from lignin.[31] A. K. Deepa and Paresh L. Dhepe carried out solid acid-catalyzed lignin depolymerization to obtain value-added aromatic monomers.[32] A. Toledano reduced lignin repolymerization by improving base-catalyzed depolymerization.[33] However, in recent years, researchers have found that combining various catalytic methods at the same time can afford better lignin depolymerization results. S. Riyang employed an acid catalyst, $CrCl_3$, and a hydrogenation catalyst, Pd/C, together to convert lignin into low molecular weight products.[34] H. Ma employed Ni/ZrP in his work.[35] Y. Fei used MoC_{1-x} and Cu–$MgAlO_z$ in lignin depolymerization.[36] Limarta used Ru/C and MgO/ZrO_2 and L. Jinxing used Ru/C and NaOH in lignin degradation.[37,38] In the above examples, the researchers combined acid catalysis and hydroprocessing,[34,36] and other studies combined base catalysis and hydroprocessing.[37,38] There are reports of joint use of acid catalysis and oxidation[39,40] and the use of base catalysis and oxidation.[41,42] Some of these results are shown in Table S8.† Compared with this work, our work has some unique advantages (as shown in Part 3.7).

From previous work, it is known that both acid and base catalytic methods are helpful in lignin depolymerization, and the combination of different catalytic methods may be more effective for lignin depolymerization.[23,35,37] However, there have been few studies about utilizing combined acid and base catalysts for lignin depolymerization. In this work, acid and base catalysts were combined in a synthesized catalyst, $S_2O_8^{2-}$–K_2O/TiO_2. The effects of the acid and base sites, temperature, and reaction time were investigated. However, in this bond breaking process, many highly reactive carbon intermediates were produced, which can easily polymerize. Because hydroprocessing is known to reduce repolymerization, it was employed in this study after $S_2O_8^{2-}$–K_2O/TiO_2 was modified by Ni. The effects of the solvent type were also studied in this work because the solvent greatly affects these kinds of studies.[43,44]

2. Materials and methods

2.1 Materials

Kraft lignin (Indulin AT™) was purchased from MeadWestvaco (Wuxi, China). Indulin AT is a kind of kraft lignin. Indulin AT is obtained from pine and has been commercialized by MeadWestvaco for the past 60 years; it is precipitated from the black liquor of linerboard grade pulp. The main characteristics of Indulin AT™ are shown in the ESI.† As shown in Table S3,† there are only 8.2 β-O-4′ per 100 Ar in Indulin AT™, compared with 41 β-O-4′ in pine-milled wood lignin. Indulin AT™ is a type of lignin which is relatively difficult to depolymerize.

$(NH_4)_2S_2O_8$, acetophenone, phenol, 2-methoxyphenol, veratrole, 4-ethylphenol, 4-methylguaiacol, 3,4-dimethoxytoluene, 4-ethylguaiacol, syringol, eugenol, 4-propylguaiacol, vanillin, isoeugenol, acetovanillone, 2,6-di-*tert*-butyl-4-methylphenol, 4-hydroxyl-3-methoxypropiophenone and homovanillic acid were bought from Aladdin. TiO_2, methanol, tetrahydrofuran, formic acid, potassium nitrate, 1,4-dioxane, $Ni(NO_3)_2 \cdot 6H_2O$ and petroleum ether (PE) were analytical grade reagents and were bought from SCR Co., Ltd. All chemicals were used without purification.

2.2 Preparation of catalysts

The $S_2O_8^{2-}$–K_2O/TiO_2 catalyst was prepared by the impregnation method. $S_2O_8^{2-}$–K_2O/TiO_2 modified by 5% Ni was prepared by the same method with an additional step of adding 0.2477 g $Ni(NO_3)_2 \cdot 6H_2O$ to the distilled water. The details are shown in the ESI (Preparation of catalysts section).†

2.3 Depolymerization of lignin

The experimental procedure is shown in the ESI (Depolymerization of lignin section).† The product distribution was measured and the HHV of the liquid product was analyzed.[45,46] The monomers were investigated by GC-MS and GC. The details of the above characterization methods are also shown in the ESI.†

2.4 Analytical methods

The surface morphology of the catalyst was investigated by a scanning electron microscope (SEM) (SIRION 200, FEI, America), and its elemental analysis was performed using an energy dispersive spectrometer (EDS, SIRION 200, FEI, America).

NH_3-temperature programmed desorption (NH_3-TPD) and CO_2-temperature programmed desorption (CO_2-TPD) measurements were carried out on an automatic chemical adsorption instrument (Quantachrome Instruments, American). 100 mg of catalyst sample was pretreated in a flow of helium (30 mL min^{-1}) at 300 °C for 1 hour, and after cooling to 100 °C, it was saturated with 6% NH_3/He (10% CO_2/He) at 300 °C. Subsequently, the excess physically adsorbed ammonia was removed by purging with helium at a flow rate of 30 mL min^{-1} at 100 °C. Lastly, the desorption process started and the temperature rose to 1200 °C at a rate of 20 °C min^{-1}. The highest permitted temperature of the instrument is 1200 °C; also, because high temperature is harmful, the NH_3-TPD and CO_2-TPD were subjected to a temperature of 1100 °C. This had no effect on the results.

H_2-temperature programmed reduction (H_2-TPR) was carried out on the same automatic chemical adsorption instrument. 100 mg of catalyst sample was pretreated in a flow of argon (30 mL min^{-1}) at 300 °C for 1 hour. After cooling to 25 °C, the reduction process started with 10% H_2/Ar at a flow rate of 30 mL min^{-1}, and the temperature rose to 550 °C at a rate of 10 °C min^{-1}.

X-ray powder diffraction (XRD) patterns were obtained with a TTR-III instrument (Rigaku Corporation, Japan). All the XRD peaks were assigned according to Joint Committee on Powder Diffraction Standards (JCPDS) cards.

3. Results and discussion

3.1 Catalyst characterization

The SEM images of TiO_2 and $S_2O_8^{2-}$–K_2O/TiO_2 are shown in Fig. S1a and b.† It can be seen that the average particle sizes

were similar, and there was no obvious agglomeration phenomenon after loading $S_2O_8^{2-}$ and K_2O. The EDS results are shown in Fig. S1c.† Pt and Cu were added to increase the surface conductivity of the catalyst to ensure its clarity when investigated by SEM. The data showed that the catalyst contained Ti, O, K, S, and there was no N. This can be explained by the fact that KNO_3 was converted into K_2O after calcination, and it can be seen that K_2O and $S_2O_8^{2-}$ were successfully loaded.

Tables S5 and S6† show the acid and base sites measured using the automatic chemical adsorption instrument (more details are shown in Fig. S2 and S3†). In general, the temperature where the peak of the acid sites appears represents the strength of the acid sites, and a higher temperature represents stronger acid sites.[47] Therefore, from Table S5,† there are 3 kinds of acid sites, namely weak acid (WA), strong acid (SA) and super strong acid (SSA), whose peaks occur at about 200 °C, 800 °C and 1100 °C, respectively. The desorbed amount of the peak represents the amount of corresponding acid sites. It is known that when only $S_2O_8^{2-}$ is present, two acid sites appear. Peaks 1 and 2, which occur at 255 °C and 730 °C, are expected to be a WA and SA, respectively. With only K_2O on the support, there is only one peak at 720 °C, which represents an SA. Because the area under the peak is large, this catalytic configuration has a large quantity of active sites. Meanwhile, it can be seen that the acidity of the catalyst was enhanced after both $S_2O_8^{2-}$ and K_2O were loaded because a SSA peak emerged. The table indicates that both $S_2O_8^{2-}$ and K_2O can increase the desorbed amount and number of SA active sites. Meanwhile, the increasing load of K_2O on the support decreased the desorbed amount and temperature of WA, but it increased the temperature of the SA. Increasing the load of $S_2O_8^{2-}$ also increased the temperature of the SA. This proves that increasing the loading of $S_2O_8^{2-}$ and K_2O can enhance the acidity of SA. When the compositions of $S_2O_8^{2-}$ and K_2O in the catalyst were both 40%, an SSA emerged at 1020 °C. Because the highest permitted temperature of the instrument is 1200 °C, only a small part of this SSA peak could emerge, and the peak temperature was higher than those of the SA and WA (shown in Fig. S2†). The desorbed amount of the appeared partial peak of 40% $S_2O_8^{2-}$–40% K_2O/TiO_2 was 653.24 μmol g^{-1}. This represents stronger acid sites and more active sites. Additionally, from the data of 20% $S_2O_8^{2-}$–20% K_2O/TiO_2, the 1 : 1 ratio of $S_2O_8^{2-}$ and K_2O may be responsible for the emergence of a SSA. Table S6† shows 3 kinds of base sites, namely weak base (WB), strong base (SB) and super strong base (SSB), at about 250 °C, 750 °C, and 1000 °C, respectively. With only $S_2O_8^{2-}$, there were two base sites at 260 °C and 755 °C, and with only K_2O, a peak was obtained at 690 °C. Although there was a difference in the desorbed amounts using NH_3-TPD and CO_2-TPD, similar trends were obtained with the two methods. Therefore, the explanation for the quantification of the base sites is similar to that of the acid sites. $S_2O_8^{2-}$ and K_2O can both enhance the SB, and a SSB appeared when $S_2O_8^{2-}$ and K_2O were loaded at the same time. It should be noted that the peaks of the acid and base sites appeared under similar conditions. According to X. Zhang's paper,[49] the Lewis acids and Lewis bases come in pairs. For example, in the Ti–O bond, the O part can provide a lone pair electron as a Lewis base and the Ti part contains a vacant site to receive a lone pair electron as a Lewis acid. Then, from W. Liu's paper,[48] these phenomena can be explained by the formation of S–O–Ti and K–O–Ti bonds by $S_2O_8^{2-}$ and K_2O; this then changed the properties of Ti–O, resulting in the emergence and enhancement of stronger acid and base sites.

The acidity and H_2-absorption capacity of the Ni-modified catalyst were characterized and compared. The results are shown in Fig. 1. Generally speaking, the Ni modifying method can improve the H_2-absorption capacity and enhance the hydrogenation ability of a catalyst. However, from Fig. 1a, it can be seen that the acidity of the catalyst was enhanced after Ni modification. Comparing lines 2 and 3, Ni–40% $S_2O_8^{2-}$–40% K_2O/TiO_2 obviously desorbed more NH_3 than 40% $S_2O_8^{2-}$–40% K_2O/TiO_2 between 150 °C and 750 °C. This proves the conclusion. From Fig. 1b, it can be easily found that Ni–40% $S_2O_8^{2-}$–40% K_2O/TiO_2 had stronger H_2-absorption capacity than 40%

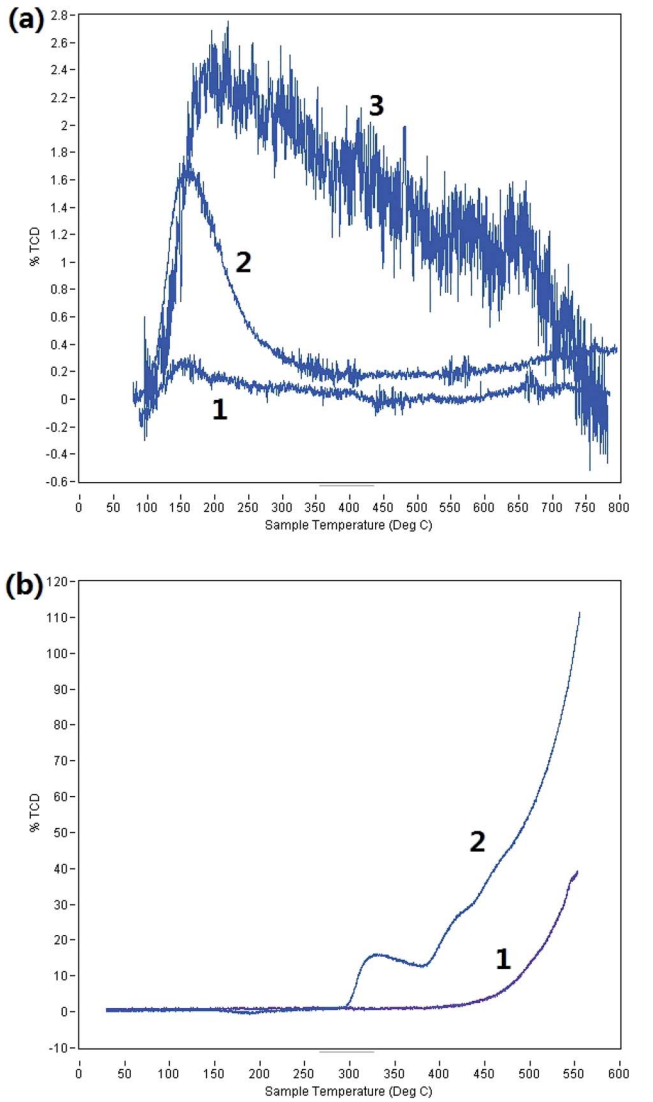

Fig. 1 (a) NH_3-TPD images (1: TiO_2; 2: 40% $S_2O_8^{2-}$–40% K_2O/TiO_2; 3: Ni–40% $S_2O_8^{2-}$–40% K_2O/TiO_2). (b) H_2-TPR images (1: 40% $S_2O_8^{2-}$–40%K_2O/TiO_2; 2: Ni–40% $S_2O_8^{2-}$–40% K_2O/TiO_2).

$S_2O_8^{2-}$–40% K_2O/TiO_2. In summary, the Ni modifying method can both enhance the hydrogenation ability and the acidity of the catalyst.

Fig. S4† shows the XRD patterns of the catalysts. The purchased untreated TiO_2 was all in anatase tetragonal phase (a). After 40% K_2O was loaded, in addition to the peak of tetragonal TiO_2 (a), new peaks of $K_2Ti_2O_5$ (b), $K_2Ti_8O_{17}$ (c) and $K_2Ti_6O_{13}$ (d) appeared. These peaks definitely indicate that the K and Ti combined through K–O–Ti bonds and new crystal structures were formed. After TiO_2 was modified by $S_2O_8^{2-}$, there were no obvious changes in its crystal structure. When $S_2O_8^{2-}$ and K_2O were loaded at the same time, a surprising result was obtained. Not only did new peaks of K_2SO_4 (e) appear, but an orthorhombic TiO_2 (f) diffraction peak appeared. The amounts of $S_2O_8^{2-}$ and K_2O obviously affected the intensity of the peaks of brookite orthorhombic TiO_2 (d). The peak of orthorhombic TiO_2 (d) was more intense than that of tetragonal TiO_2 (a) after loading 40% $S_2O_8^{2-}$ and 40% K_2O on TiO_2. Considering the TPD results, the formation of new peaks for orthorhombic TiO_2 (d) and K_2SO_4 (e) may be related to the enhancement of the acid and base sites. From Table 2, K_2SO_4/TiO_2 showed poor catalytic properties. Thus, the transformation of tetragonal and orthorhombic TiO_2 probably has a correlation with the enhancement of the acid and base sites. Additionally, according to the figure, loading Ni had no obvious effect on the XRD pattern of the catalyst. The specific JCPDS file numbers for the peaks are provided in the ESI.†

3.2 Effects of the solvent

The effects of the solvent type were researched. The results are shown in Table 1. The experiments were performed at 320 °C, and the reaction time was 1 h. Different solvents were used in the reaction. 1,4-Dioxane and another chemical reagent (methanol, formic, water or tetrahydrofuran) were mixed as composite solvents. The volume of 1,4-dioxane was fixed in the reaction, while that of the other chemical reagent was varied. Different ratios of the two constituent solvents were used to ensure that lignin completely dissolved in the resulting solvent. The yield of liquid product reflected the liquefaction degree of lignin depolymerization. The yield of solid product represented the condensation degree of lignin depolymerization during the reaction. In the process of lignin depolymerization, polycondensation of the degradation products also occurs. The solid products are mainly polycondensates of the degradation products.[23] According to Jiang,[50] the PE-soluble product consists of monomers, dimers, trimers and slightly larger multimers because its number-average molecular weight is about 364. Thus, the yield of PE-soluble product represents the depolymerization degree of lignin. That is, the more PE-soluble the product, the better the efficiency of lignin depolymerization.

Table 1 shows that the choice of solvent can exert an influence on lignin depolymerization, and four different solvents were investigated. When 1,4-dioxane/methanol and 1,4-dioxane/formic acid were used, the yields of liquid product were 72.23% and 72.87%, respectively; these are higher than those of 1,4-dioxane/water and 1,4-dioxane/tetrahydrofuran (69.76% and 70.13%, respectively). This demonstrates that methanol and formic acid can promote lignin depolymerization to a degree, and these two reagents played different roles in the reaction. Methanol is the hydrogen donor, and it can reduce repolymerization.[27,44] Because formic acid is unstable at high temperatures and will decompose to form carbon dioxide and hydrogen when the temperature rises over 160 °C, it can only promote lignin depolymerization at low temperatures. The yield of PE-soluble product was highest at 40.54% with 1,4-dioxane/methanol; this was markedly higher than the other yields. These results show that methanol can promote lignin depolymerization as the hydrogen donor solvent. Due to the reasons above, 1,4-dioxane/methanol was chosen as the solvent in the following experiments.

3.3 Effects of the acid and base sites on lignin depolymerization

The catalytic lignin depolymerization results are shown in Table 2. From Tables S5, S6† and 2, increasing the loading of K_2O decreased the temperatures of the WA and WB sites, and the liquid product yield decreased from 95.28% to 67.44%. These results indicate that the strengths of WA and WB are negatively correlated with char formation. Meanwhile, the yield of the residue increased from 3.99% to 31.89%. A similar trend was observed when $S_2O_8^{2-}$ was decreased; it was found that the yield of the liquid product declined from 67.44% to 38.32%. The decreased loading of $S_2O_8^{2-}$ and increased loading of K_2O may have enhanced the char formation and diminished the yield of the liquid product. Because the PE-soluble product comprised low molecular weight compounds, the amount of PE-soluble product can better represent the degree of lignin depolymerization. From Table 2, it can be seen that the highest yield (22.86%) of the PE-soluble product was obtained with the use of 40% $S_2O_8^{2-}$–40% K_2O/TiO_2, the strongest acid–base catalyst formulation. When the loading amounts of $S_2O_8^{2-}$ and K_2O were 20%, an acceptable result (17.1%) of PE-soluble product

Table 1 Effects of the solvent and product distributions[a]

Solvent	Liquid product/%	Solid product/%	Gas product/%	PE-soluble product/%
30 mL 1,4-dioxane and 1 mL distilled water	69.76 ± 2.37	24.99 ± 1.37	5.25 ± 1.04	31.25 ± 3.15
30 mL 1,4-dioxane and 6 mL methanol	65.23 ± 1.92	30.04 ± 2.14	4.73 ± 1.84	40.54 ± 2.83
30 mL 1,4-dioxane and 0.5 mL tetrahydrofuran	70.13 ± 1.41	23.93 ± 2.93	5.94 ± 0.69	33.86 ± 1.77
30 mL 1,4-dioxane and 3 mL formic acid	72.87 ± 3.12	21.71 ± 2.06	5.42 ± 1.13	33.49 ± 2.36

[a] Conditions: 0.5 g lignin, 0.2 g catalyst, 4 MPa H_2, 320 °C, 1 h, 900 rpm.

Table 2 Effects of the acid and base sites and product distributions[a]

Catalyst	Liquid product/%	Solid product/%	Gas product/%	PE-soluble product/%
40% $S_2O_8^{2-}$–0% K_2O/TiO_2	95.28 ± 2.04	3.99 ± 1.47	0.73 ± 0.52	12.16 ± 0.87
40% $S_2O_8^{2-}$–20% K_2O/TiO_2	78.38 ± 1.83	20.5 ± 1.22	1.12 ± 0.60	15.38 ± 0.93
40% $S_2O_8^{2-}$–40% K_2O/TiO_2	67.44 ± 1.57	31.01 ± 2.28	1.55 ± 0.35	22.86 ± 1.04
20% $S_2O_8^{2-}$–40% K_2O/TiO_2	43.94 ± 2.62	54.12 ± 1.73	1.94 ± 0.52	14.28 ± 2.01
0% $S_2O_8^{2-}$–40% K_2O/TiO_2	38.32 ± 1.87	59.9 ± 1.07	1.78 ± 0.62	11.9 ± 1.32
20% $S_2O_8^{2-}$–20% K_2O/TiO_2	76.06 ± 3.10	22.96 ± 2.61	0.98 ± 0.73	17.1 ± 2.18
40% K_2SO_4/TiO_2	78.90 ± 1.95	20.06 ± 1.40	1.04 ± 0.42	7.42 ± 2.07

[a] Conditions: 0.5 g lignin, 0.2 g catalyst, 30 mL 1,4-dioxane and 6 mL methanol, 4 MPa H_2, 280 °C, 1 h, 900 rpm.

was obtained. This demonstrates that the influence of the strength is greater than that of the amount. From Fig. S4,† when $S_2O_8^{2-}$ and K_2O were loaded at the same time, some K_2SO_4 was generated. However, the last entry in Table 2 shows that K_2SO_4 had poor catalytic properties. These results definitely prove the importance of using a solid super acid–base composite with an appropriate loading amount.

3.4 Effects of temperature on lignin depolymerization

The effects of temperature on lignin depolymerization were also studied. The reaction was carried out at different temperatures (260 °C, 280 °C, 300 °C and 320 °C), and the other conditions were the same as above except for the solvent type. Because tetrahydrofuran is harmful to health and formic acid is unstable, 1,4-dioxane/water and 1,4-dioxane/methanol were chosen as solvents. The effects of temperature in 1,4-dioxane/water are shown in Fig. 2a, and the effects of temperature in 1,4-dioxane/methanol are shown in Fig. 2b. From Fig. 2, it can be seen that the yield of liquid product in 1,4-dioxane/water increased as the temperature changed from 260 °C to 280 °C (73.78% to 78.86%); the yield then decreased to 320 °C (69.76%). However, in 1,4-dioxane/methanol, increasing the temperature diminished the liquid product from 70.52% to 61.58%. Unlike the results of the liquid product, the PE-soluble product variations were similar in the two solvents. The yields of PE-soluble product rose markedly from 260 °C to 320 °C (1,4-dioxane/water: 6.85% to 31.25%; 1,4-dioxane/methanol: 12.96% to 40.54%). From the figures, it can be easily seen that the yield of PE-soluble product was obviously higher with 1,4-dioxane/methanol than with 1,4-dioxane/water as the solvent. This indeed shows that a hydrogen-donating reagent can promote lignin depolymerization. Additionally, high temperatures afforded more gas product. For 1,4-dioxane/water, the gas product yield increased from 2.24% to 5.25%, while for 1,4-dioxane/methanol, it increased from 0.67% to 4.73% when the temperature increased from 260 °C to 320 °C. Generally, high temperatures can promote lignin depolymerization.

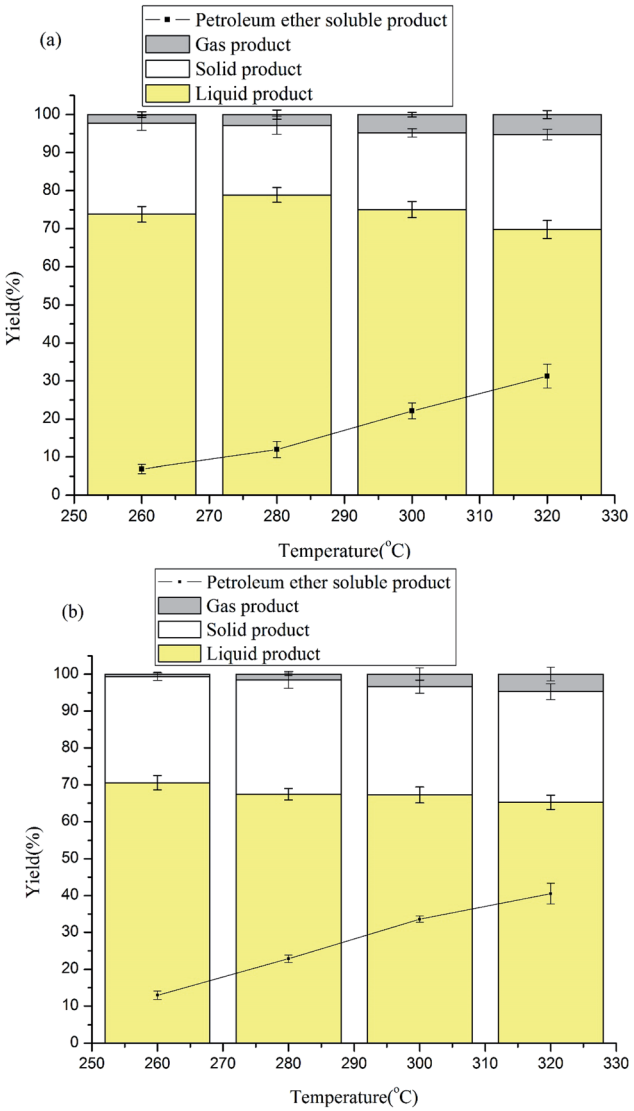

Fig. 2 Effects of temperature and product distribution. (a) The solvent was 1,4-dioxane/water. (b) The solvent was 1,4-dioxane/methanol. Other conditions: 0.5 g lignin, 0.2 g catalyst, 4 MPa H_2, 1 h, 900 rpm.

3.5 Effects of reaction time

The effects of the reaction time were researched. The experiments were performed at 260 °C and 320 °C in 1,4-dioxane/methanol with $S_2O_8^{2-}$–K_2O/TiO_2 for different reaction times (1, 6, 12 and 24 h). The resulting data of the experiment are shown in Fig. 3. Fig. 3a shows the results at 260 °C with $S_2O_8^{2-}$–K_2O/TiO_2 and Fig. 3b shows those at 320 °C with $S_2O_8^{2-}$–K_2O/TiO_2. Fig. 3a shows that when using $S_2O_8^{2-}$–K_2O/TiO_2 at 260 °C, prolonging the reaction time did not favour the yield of liquid product (1 h to 24 h: 70.52% to 61.58%) but enhanced the formation of PE-

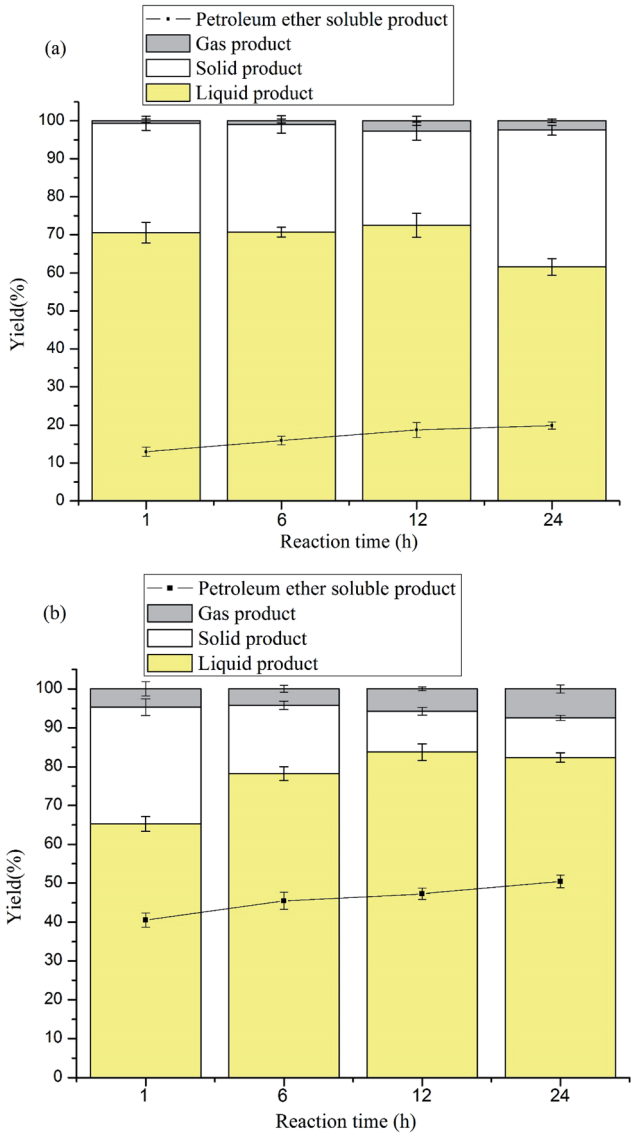

Fig. 3 Effects of reaction time and product distribution. (a) The reaction was performed with $S_2O_8^{2-}$–K_2O/TiO_2 at 260 °C. (b) The reaction was performed with $S_2O_8^{2-}$–K_2O/TiO_2 at 320 °C. Other conditions: 0.5 g lignin, 0.2 g catalyst, 30 mL 1,4-dioxane and 6 mL methanol, 4 MPa H_2, 1 h, 900 rpm.

soluble product (1 h to 24 h: 12.96% to 19.88%). However, from Fig. 3b, the two yields (liquid and PE-soluble product) increased from 65.23% and 40.54% to 82.4% and 50.4%, respectively. It can be seen from the two figures that extending the reaction time could depolymerize lignin better and increase the yield of the PE-soluble product. It should also be noted that $S_2O_8^{2-}$–K_2O/TiO_2 has the ability to stabilize the intermediate and reduce char formation at high temperatures (about 320 °C). Hence, prolonging the reaction time can facilitate lignin depolymerization and produce more monomers and dimers.

3.6 Effects of Ni-modified catalyst

The experiment was performed at 260 °C and 320 °C in 1,4-dioxane/methanol with Ni–$S_2O_8^{2-}$–K_2O/TiO_2 for different reaction times (1, 6, 12 and 24 h). The results of the experiment are shown in Fig. 4. Fig. 4a shows the results at 260 °C with Ni–$S_2O_8^{2-}$–K_2O/TiO_2 and Fig. 4b shows those at 320 °C with Ni–$S_2O_8^{2-}$–K_2O/TiO_2. Fig. 4a shows that when Ni–$S_2O_8^{2-}$–K_2O/TiO_2 was used at 260 °C, prolonging the reaction time increased the yield of the liquid product and PE-soluble product from 60.22% and 23.51% to 77.68% and 31.24%, respectively. This can be explained by the fact that the enhanced acidity rapidly promoted the reaction degree and afforded more char and more PE-soluble product. However, the hydrogenation was correspondingly slow, and more time was needed to stabilize the reaction intermediate. At a higher temperature (320 °C), this phenomenon was more obvious. As shown in Fig. 4b, the two yields increased from 50.32% and 41.08% to 70.12% and 56.4%,

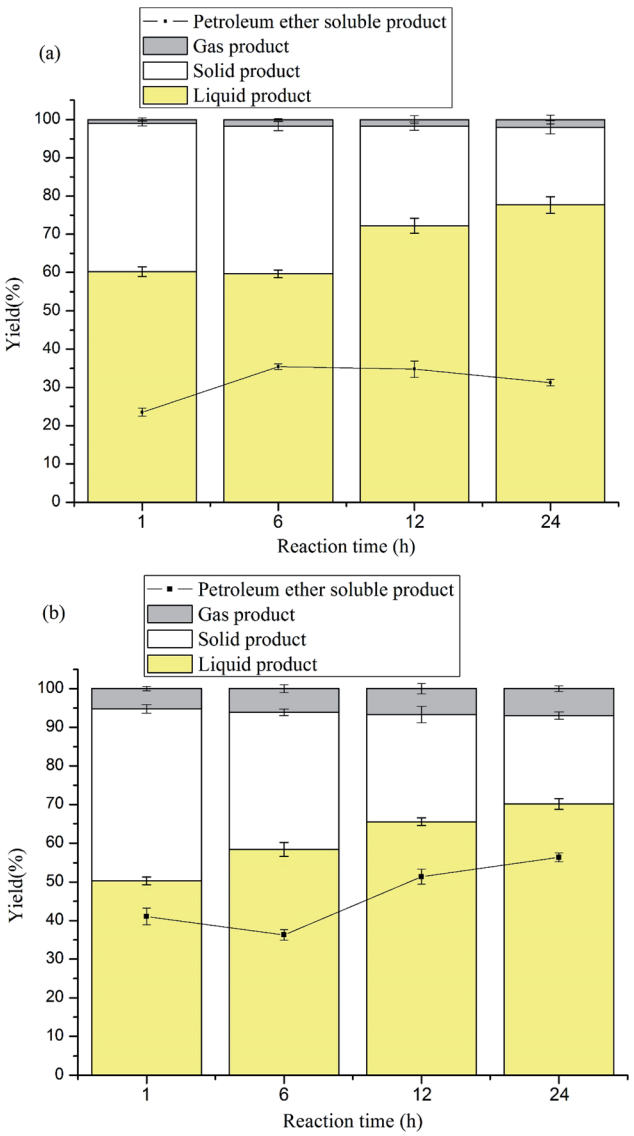

Fig. 4 Effects of the Ni-modified catalyst and product distribution. (a) The reaction was performed with Ni–$S_2O_8^{2-}$–K_2O/TiO_2 at 260 °C. (b) The reaction was performed with Ni–$S_2O_8^{2-}$–K_2O/TiO_2 at 320 °C. Other conditions: 0.5 g lignin, 0.2 g catalyst, 30 mL 1,4-dioxane and 6 mL methanol, 4 MPa H_2, 1 h, 900 rpm.

respectively, when the reaction time was extended to 24 h. From Fig. 3a and 4a, it can be found that the Ni-modified catalyst had obvious effects and effectively increased the two yields. At 260 °C and 24 h, the two yields increased from 61.58% and 19.88% to 77.68% and 31.24%, respectively, for the catalyst modified by Ni. It can be seen from Fig. 3b and 4b that the two catalysts led to similar results, in which extending the reaction time at 320 °C reduced char formation and increased the yield of the other products. However, the Ni-modified catalyst caused about 10% lowering of the yield of liquid product and increased the yield of PE-soluble product by about 6%. Comparing the results of the two catalysts ($S_2O_8^{2-}$–K_2O/TiO_2 and Ni–$S_2O_8^{2-}$–K_2O/TiO_2) at different temperatures, it can be seen that the performance of Ni–$S_2O_8^{2-}$–K_2O/TiO_2 was obviously more effective at 260 °C than at 320 °C. Combined with the conclusions in Section 3.1 and Fig. 1, this can be explained by the fact that the Ni modifying process enhanced the hydrogenation ability and the acidity of the catalyst. The stronger acidity promotes the reaction degree and the enhanced hydrogenation ability stabilizes the reaction intermediate well after prolonging the reaction time at 260 °C. However, at 320 °C, the reaction degree was sufficiently strong. Then, the reaction promoted by the stronger acidity led to more char formation, and the enhanced hydrogenation ability could not sufficiently stabilize the reaction intermediate. Meanwhile, the stronger reaction and enhanced hydrogenation afforded more micromolecular products and PE-soluble product. In total, increasing the acidity of the catalyst will promote the reaction degree, and the hydrogenation will stabilize the reaction intermediate. However, at high temperature (about 320 °C), the acidity of the catalyst should be limited and the hydrogenation ability should be enhanced as much as possible.

3.7 The analysis of liquid product

The results of the GC-MS analysis are shown in Fig. S5.† According to the GC-MS analysis, the monomer products were phenol, 2-methoxyphenol, veratrole, 4-ethylphenol, 4-methylguaiacol, 3,4-dimethoxytoluene, 4-ethylguaiacol, syringol, eugenol, 4-propylguaiacol, vanillin, isoeugenol, acetovanillone, 2,6-di-*tert*-butyl-4-methylphenol, 4-hydroxyl-3-methoxypropiophenone and homovanillic acid. Other products could not be identified because they have many isomers and too many possible structural formulas. Another reason that these products could not be identified and quantified is that their standard samples cannot be purchased. Thus, the yields of unknown monomers were calculated by the mean of the correcting coefficients of the known monomers. The GC results of the monomer products are shown in Table 3 (the details are shown in Table S7†). From the results, it can be seen that the yield of total monomers increased obviously after increasing the temperature and prolonging the reaction time. When the reaction time was short (1 h), the ratio of the yields of identified monomers (mainly guaiacol and some derivates) and total monomers was greater than the ratio of the yields at 12 h. This indicates that a short reaction time benefits the formation of guaiacol and some derivates, and the simple identified monomers become more complex with increasing reaction time. When the reaction time was prolonged from 1 h to 12 h at 320 °C, the decrease of the yield of 2-methoxy-phenol supported this opinion. In summary, increasing the reaction temperature and prolonging the reaction time increased the yield of total monomers; however, a long reaction time affords more complex monomer products.

Table 4 shows the elemental contents of the liquid product and PE-soluble product. The results show that the amount of oxygen decreased while those of carbon and hydrogen increased after the reaction. Meanwhile, the reaction also reduced the S content. The N content changed slightly after the lignin depolymerization reaction. As shown in Table 4, increasing both the reaction temperature and the reaction time promoted hydrodeoxygenation and desulfuration. Meanwhile, the HHV increased. At 260 °C and 1 h, the HHV increments are 1.2 MJ kg^{-1} (25.7 to 26.9) and 2.0 MJ kg^{-1} (25.7 to 27.7). However, at 320 °C and 24 h, the respective increments are much greater: 7.1 MJ kg^{-1} (25.7 to 32.8) and 7.9 MJ kg^{-1} (25.7 to 33.6). The table also demonstrates that the Ni-modified catalytic system promoted the hydrodeoxygenation ability of the catalyst. Under most conditions, the liquid product obtained with the Ni-modified catalyst included more H content and less O content and increased the HHV. Additionally, it can be found that the HHV of the PE-soluble product was obviously higher than that of the liquid product from the same depolymerization reaction. The highest HHV (37.4 MJ kg^{-1}) was obtained with Ni–$S_2O_8^{2-}$–K_2O/TiO_2 at 320 °C and 24 h.

In order to better illustrate the advantages of $S_2O_8^{2-}$–K_2O/TiO_2, a comparison of its lignin depolymerization performance with the literature is summarized in Table S8.† It can be easily found that $S_2O_8^{2-}$–K_2O/TiO_2 shows comparable catalytic

Table 3 The GC results of the monomer products[a]

Catalyst	Reaction time	Reaction temperature	Total unknown monomers/%	Total identified monomers/%	Total monomers/%
$S_2O_8^{2-}$–K_2O/TiO_2	1 h	260 °C	6.78 ± 0.17	3.01 ± 0.12	9.79 ± 0.22
Ni–$S_2O_8^{2-}$–K_2O/TiO_2	1 h	260 °C	5.43 ± 0.29	3.10 ± 0.09	8.53 ± 0.37
$S_2O_8^{2-}$–K_2O/TiO_2	1 h	320 °C	7.56 ± 0.41	5.81 ± 0.35	13.37 ± 0.62
Ni–$S_2O_8^{2-}$–K_2O/TiO_2	1 h	320 °C	7.43 ± 0.26	7.52 ± 0.42	14.95 ± 0.57
$S_2O_8^{2-}$–K_2O/TiO_2	12 h	320 °C	20.07 ± 0.64	8.89 ± 0.41	28.96 ± 0.72
Ni–$S_2O_8^{2-}$–K_2O/TiO_2	12 h	320 °C	17.17 ± 0.52	7.80 ± 0.50	24.97 ± 0.83

[a] Conditions: 0.5 g lignin, 0.2 g catalyst, 4 MPa H_2, 900 rpm.

Table 4 Elemental contents after the reactions[a]

	Catalyst	Reaction temperature	Reaction time	Elemental content (wt%) C	H	O	N	S	HHV (MJ kg^{-1})
Indulin AT	—	—	—	65.5	5.6	25.2	0.4	3.3	25.7
Liquid product	$S_2O_8^{2-}$–K_2O/TiO_2	260 °C	1 h	65.4	6.5	24.8	0.6	2.7	26.9
	Ni–$S_2O_8^{2-}$–K_2O/TiO_2	260 °C	1 h	65.3	7.0	24.5	0.4	2.8	27.7
	$S_2O_8^{2-}$–K_2O/TiO_2	260 °C	24 h	69.1	6.8	21.2	0.6	2.3	29.2
	Ni–$S_2O_8^{2-}$–K_2O/TiO_2	260 °C	24 h	69.2	7.1	21.1	0.5	2.1	29.6
	$S_2O_8^{2-}$–K_2O/TiO_2	320 °C	1 h	69.5	7.1	21.7	0.6	1.1	29.5
	Ni–$S_2O_8^{2-}$–K_2O/TiO_2	320 °C	1 h	70.1	6.9	21.4	0.4	1.2	29.5
	$S_2O_8^{2-}$–K_2O/TiO_2	320 °C	24 h	71.7	8.5	18.5	0.5	0.8	32.8
	Ni–$S_2O_8^{2-}$–K_2O/TiO_2	320 °C	24 h	72.6	8.7	17.5	0.5	0.7	33.6
PE-soluble product	$S_2O_8^{2-}$–K_2O/TiO_2	320 °C	24 h	70.7	10.7	17.9	0.4	0.3	35.7
	Ni–$S_2O_8^{2-}$–K_2O/TiO_2	320 °C	24 h	70.3	11.9	17.2	0.4	0.2	37.4

[a] Conditions: 0.5 g lignin, 0.2 g catalyst, 4 MPa H_2, 900 rpm.

performance to these catalysts. Compared with the catalysts in ref. 34, 35 and 37, the reaction temperature and time are higher, but the yield of monomer products is also higher. Additionally, from Limarta's work,[38] it is known that organosolv lignin has higher depolymerization efficiency due to its less condensed structure and the absence of catalyst-poisoning sulfur. Another advantage of $S_2O_8^{2-}$–K_2O/TiO_2 is that there is no noble metal in the catalyst; therefore, the catalyst is inexpensive to prepare. The comparison results show that $S_2O_8^{2-}$–K_2O/TiO_2 is an efficient, inexpensive and high-industrial-value catalyst.

3.8 Stability examination of $S_2O_8^{2-}$–K_2O/TiO_2 and Ni–$S_2O_8^{2-}$–K_2O/TiO_2

Catalyst stability is significant to consider before adopting a catalyst on a large scale. To investigate the stabilities of $S_2O_8^{2-}$–K_2O/TiO_2 and Ni–$S_2O_8^{2-}$–K_2O/TiO_2, 2 reactions were performed at 260 °C; the other conditions were 0.5 g lignin, 0.2 g catalyst, 4 MPa H_2, 1 h, and 900 rpm. The results are shown in Fig. 5. After every cycle, the catalyst was filtered, washed with acetone and then dried in an oven. The results for $S_2O_8^{2-}$–K_2O/TiO_2 showed that the catalyst has acceptable stability. After 5 cycles, the effects of the catalyst decreased by about 25% and the yields of liquid product and PE-soluble product decreased from 70.52% and 12.96% to 50.69% and 8.42%, respectively. From the figure, it can be found that the Ni modification stabilized the catalyst and reduced the 25% loss to about 17%. The yields of liquid product and PE-soluble product changed from 60.22% and 23.51% to 51.37% and 18.67%, respectively.

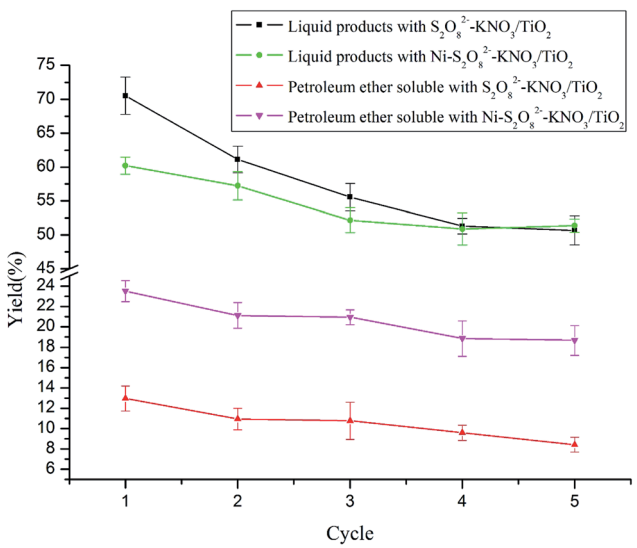

Fig. 5 Results of the stability tests of the catalysts.

4. Conclusion

Here, a dual property (acid and base) catalyst, $S_2O_8^{2-}$–K_2O/TiO_2, was carefully researched, and the effects of the acid and base sites, solvent, temperature and reaction time on lignin depolymerization were investigated. The Ni-modified catalyst and the effects of its acidity and hydrogenation capacity were also researched. From the NH_3-TPD, CO_2-TPD and H_2-TPR results, it was found that loading $S_2O_8^{2-}$ and K_2O together could immensely strengthen the acid and base sites of the catalyst and effectively facilitate lignin depolymerization; also, Ni modification could enhance the acidity and hydrogenation capacity. In this research, it was found that 1,4-dioxane/methanol promoted lignin depolymerization better than the other solvents. To obtain better depolymerization results, a higher temperature (about 320 °C) and longer reaction time (at least 12 h) are necessary; this can obviously promote hydrodeoxygenation and desulfuration. In the presence of hydrogen, the Ni-modified method can effectively promote the catalytic activity and stabilize the catalyst. Under appropriate conditions, the yields of liquid product, PE-soluble product and total monomer products were 82.4%, 50.4% and 28.96%, respectively, and the HHV of the liquid product was 32.8 MJ kg^{-1}. In addition, after the catalyst was modified by Ni, the yield of PE-soluble product increased to 56.4%, while the highest product HHV (33.6 MJ kg^{-1}) was obtained after the reaction.

Conflicts of interest

There are no conflicts to declare.

Acknowledgements

This study was financially supported by the Program of National Natural Science Foundation of China (51976212), the National Key R&D Program of China (No. 2018YFB1501601) and "Transformational Technologies for Clean Energy and Demonstration", Strategic Priority Research Program of the Chinese Academy of Sciences, Grant No. XDA 21060101.

References

1 S. Wang, G. Dai, H. Yang and Z. Luo, Lignocellulosic biomass pyrolysis mechanism: a state-of-the-art review, *Prog. Energy Combust. Sci.*, 2017, **62**, 33–86.

2 W. Ouyang, X. Zhao, M. Tysklind, F. Hao and F. Wang, Optimisation of corn straw biochar treatment with catalytic pyrolysis in intensive agricultural area, *Ecol. Eng.*, 2015, **84**, 278–286.

3 S. Wang, Z. Li, X. Bai, W. Yi and P. Fu, Influence of inherent hierarchical porous char with alkali and alkaline earth metallic species on lignin pyrolysis, *Bioresour. Technol.*, 2018, **268**, 323–331.

4 K. Zhang, H. Li, L. P. Xiao, B. Wang, R. C. Sun and G. Song, Sequential utilization of bamboo biomass through reductive catalytic fractionation of lignin, *Bioresour. Technol.*, 2019, 121335.

5 Y. Liao, Q. Liu, T. Wang, J. Long, L. Ma and Q. Zhang, Zirconium phosphate combined with Ru/C as a highly efficient catalyst for the direct transformation of cellulose to C6 alditols, *Green Chem.*, 2014, **16**(6), 3305–3312.

6 H. Lin, J. Chen, Y. Zhao and S. Wang, Conversion of C5 carbohydrates into furfural catalyzed by SO_3H-functionalized ionic liquid in renewable γ-valerolactone, *Energy Fuels*, 2017, **31**(4), 3929–3934.

7 H. Lin, Q. Xiong, Y. Zhao, J. Chen and S. Wang, Conversion of carbohydrates into 5-hydroxymethylfurfural in a green reaction system of CO_2-water-isopropanol, *AIChE J.*, 2017, **63**(1), 257–265.

8 N. Shi, Q. Liu, Q. Zhang, T. Wang and L. Ma, High yield production of 5-hydroxymethylfurfural from cellulose by high concentration of sulfates in biphasic system, *Green Chem.*, 2013, **15**(7), 1967–1974.

9 S. Wang, Y. Zhao, H. Lin, J. Chen, L. Zhu and Z. Luo, Conversion of C5 carbohydrates into furfural catalyzed by a Lewis acidic ionic liquid in renewable γ-valerolactone, *Green Chem.*, 2017, **19**(16), 3869–3879.

10 R. Rinaldi, R. Jastrzebski, M. T. Clough, J. Ralph, M. Kennema, P. C. Bruijnincx and B. M. Weckhuysen, Paving the way for lignin valorisation: recent advances in bioengineering, biorefining and catalysis, *Angew. Chem., Int. Ed.*, 2016, **55**(29), 8164–8215.

11 J. Rencoret, A. Gutiérrez, L. Nieto, J. Jiménez-Barbero, C. B. Faulds, H. Kim, *et al.*, Lignin composition and structure in young *versus* adult Eucalyptus globulus plants, *Plant Physiol.*, 2011, **155**(2), 667–682.

12 M. Danish and T. Ahmad, A review on utilization of wood biomass as a sustainable precursor for activated carbon production and application, *Renewable Sustainable Energy Rev.*, 2018, **87**, 1–21.

13 Z. Sun, B. Fridrich, A. de Santi, S. Elangovan and K. Barta, Bright side of lignin depolymerization: toward new platform chemicals, *Chem. Rev.*, 2018, **118**(2), 614–678.

14 P. J. Deuss, M. Scott, F. Tran, N. J. Westwood, J. G. de Vries and K. Barta, Aromatic monomers by in situ conversion of reactive intermediates in the acid-catalyzed depolymerization of lignin, *J. Am. Chem. Soc.*, 2015, **137**(23), 7456–7467.

15 A. J. Ragauskas, G. T. Beckham, M. J. Biddy, R. Chandra, F. Chen, M. F. Davis, B. H. Davison, R. A. Dixon, P. Gilna, M. Keller, P. Langan, A. K. Naskar, J. N. Saddler, T. J. Tschaplinski, G. A. Tuskan and C. E. Wyman, Lignin valorization: improving lignin processing in the biorefinery, *Science*, 2014, **344**(6185), 1246843.

16 P. Azadi, O. R. Inderwildi, R. Farnood and D. A. King, Liquid fuels, hydrogen and chemicals from lignin: a critical review, *Renewable Sustainable Energy Rev.*, 2013, **21**, 506–552.

17 B. Joffres, D. Laurenti, N. Charon, A. Daudin, A. Quignard and C. Geantet, Thermochemical conversion of lignin for fuels and chemicals: a review, *Oil Gas Sci. Technol.*, 2013, **68**(4), 753–763.

18 A. Galadima and O. uraza, In situ fast pyrolysis of biomass with zeolite catalysts for bioaromatics/gasoline production: a review, *Energy Convers. Manage.*, 2015, **105**, 338–354.

19 J. Y. Kim, J. H. Lee, J. Park, J. K. Kim, D. An, I. K. Song and J. W. Choi, Catalytic pyrolysis of lignin over HZSM-5 catalysts: effect of various parameters on the production of aromatic hydrocarbon, *J. Anal. Appl. Pyrolysis*, 2015, **114**, 273–280.

20 D. Shen, J. Zhao and R. Xiao, Catalytic transformation of lignin to aromatic hydrocarbons over solid-acid catalyst: effect of lignin sources and catalyst species, *Energy Convers. Manage.*, 2016, **124**, 61–72.

21 H. Wang, Y. Pu, A. Ragauskas and B. Yang, From lignin to valuable products-strategies, challenges, and prospects, *Bioresour. Technol.*, 2019, **271**, 449–461.

22 C. Li, X. Zhao, A. Wang, G. W. Huber and T. Zhang, Catalytic transformation of lignin for the production of chemicals and fuels, *Chem. Rev.*, 2015, **115**(21), 11559–11624.

23 W. Schutyser, T. Renders, S. Van den Bosch, *et al.*, Chemicals from lignin: an interplay of lignocellulose fractionation, depolymerisation, and upgrading, *Chem. Soc. Rev.*, 2018, **47**(3), 852–908.

24 D. M. de Carvalho and J. L. Colodette, Comparative Study of Acid Hydrolysis of Lignin and Polysaccharides in Biomasses, *BioResources*, 2017, **12**(4), 6907–6923.

25 R. Katahira, A. Mittal, K. McKinney, X. Chen, M. P. Tucker, D. K. Johnson and G. T. Beckham, Base-catalyzed depolymerization of biorefinery lignins, *ACS Sustainable Chem. Eng.*, 2016, **4**(3), 1474–1486.

26 M. Tayier, D. Duan, Y. Zhao, R. Ruan, Y. Wang and Y. Liu, Catalytic Effects of Various Acids on Microwave-assisted Depolymerization of Organosolv Lignin, *BioResources*, 2017, **13**(1), 412–424.

27 K. Barta, T. D. Matson, M. L. Fettig, S. L. Scott, A. V. Iretskii and P. C. Ford, Catalytic disassembly of an organosolv lignin *via* hydrogen transfer from supercritical methanol, *Green Chem.*, 2010, **12**(9), 1640–1647.

28 X. Zhang, Q. Zhang, T. Wang, L. Ma, Y. Yu and L. Chen, Hydrodeoxygenation of lignin-derived phenolic compounds to hydrocarbons over Ni/SiO_2–ZrO_2 catalysts, *Bioresour. Technol.*, 2013, **134**, 73–80.

29 M. Grilc, B. Likozar and J. Levec, Hydrodeoxygenation and hydrocracking of solvolysed lignocellulosic biomass by oxide, reduced and sulphide form of NiMo, Ni, Mo and Pd catalysts, *Appl. Catal., B*, 2014, **150**, 275–287.

30 M. Grilc, B. Likozar and J. Levec, Kinetic model of homogeneous lignocellulosic biomass solvolysis in glycerol and imidazolium-based ionic liquids with subsequent heterogeneous hydrodeoxygenation over $NiMo/Al_2O_3$ catalyst, *Catal. Today*, 2015, **256**, 302–314.

31 Y. Ye, Y. Zhang, J. Fan and J. Chang, Selective production of 4-ethylphenolics from lignin *via* mild hydrogenolysis, *Bioresour. Technol.*, 2012, **118**, 648–651.

32 A. K. Deepa and P. L. Dhepe, Solid acid catalyzed depolymerization of lignin into value added aromatic monomers, *RSC Adv.*, 2014, **4**(25), 12625–12629.

33 A. Toledano, L. Serrano and J. Labidi, Improving base catalyzed lignin depolymerization by avoiding lignin repolymerization, *Fuel*, 2014, **116**, 617–624.

34 R. Shu, J. Long, Y. Xu, L. Ma, Q. Zhang, T. Wang, *et al.*, Investigation on the structural effect of lignin during the hydrogenolysis process, *Bioresour. Technol.*, 2016, **200**, 14–22.

35 H. Ma, H. Li, W. Zhao, L. Li, S. Liu, J. Long and X. Li, Selective depolymerization of lignin catalyzed by nickel supported on zirconium phosphate, *Green Chem.*, 2019, **21**(3), 658–668.

36 F. Yan, R. Ma, X. Ma, K. Cui, K. Wu, M. Chen and Y. Li, Ethanolysis of Kraft lignin to platform chemicals on a MoC_{1-x}/Cu-$MgAlO_z$ catalyst, *Appl. Catal., B*, 2017, **202**, 305–313.

37 J. Long, Y. Xu, T. Wang, Z. Yuan, R. Shu, Q. Zhang and L. Ma, Efficient base-catalyzed decomposition and in situ hydrogenolysis process for lignin depolymerization and char elimination, *Appl. Energy*, 2015, **141**, 70–79.

38 S. O. Limarta, J. M. Ha, Y. K. Park, H. Lee, D. J. Suh and J. Jae, Efficient depolymerization of lignin in supercritical ethanol by a combination of metal and base catalysts, *J. Ind. Eng. Chem.*, 2018, **57**, 45–54.

39 A. Rahimi, A. Ulbrich, J. J. Coon and S. S. Stahl, Formic-acid-induced depolymerization of oxidized lignin to aromatics, *Nature*, 2014, **515**(7526), 249.

40 M. Wang, L. H. Li, J. M. Lu, H. J. Li, X. C. Zhang, H. F. Liu, *et al.*, Acid promoted C–C bond oxidative cleavage of β-O-4 and β-1 lignin models to esters over a copper catalyst, *Green Chem.*, 2017, **19**(3), 702–706.

41 S. K. Hanson and R. T. Baker, Knocking on wood: base metal complexes as catalysts for selective oxidation of lignin models and extracts, *Acc. Chem. Res.*, 2015, **48**(7), 2037–2048.

42 X. Ouyang, T. Ruan and X. Qiu, Effect of solvent on hydrothermal oxidation depolymerization of lignin for the production of monophenolic compounds, *Fuel Process. Technol.*, 2016, **144**, 181–185.

43 M. Oregui-Bengoechea, I. Gandarias, P. L. Arias and T. Barth, Unraveling the role of formic acid and the type of solvent in the catalytic conversion of lignin: a holistic approach, *ChemSusChem*, 2017, **10**(4), 754–766.

44 X. Wang and R. Rinaldi, Solvent effects on the hydrogenolysis of diphenyl ether with Raney nickel and their implications for the conversion of lignin, *ChemSusChem*, 2012, **5**(8), 1455–1466.

45 M. K. Jindal and M. K. Jha, Effect of process parameters on hydrothermal liquefaction of waste furniture sawdust for bio-oil production, *RSC Adv.*, 2016, **6**(48), 41772–41780.

46 J. Yang, L. Zhao, S. Liu, Y. Wang and L. Dai, High-quality bio-oil from one-pot catalytic hydrocracking of kraft lignin over supported noble metal catalysts in isopropanol system, *Bioresour. Technol.*, 2016, **212**, 302–310.

47 K. Ren, J. Liu, X. Wang, L. Shi, X. Meng and N. Liu, Iron modified SO_4^{2-}/ZrO_2 in application of removing trace olefins from aromatics, *Pet. Sci. Technol.*, 2019, **37**(1), 8–14.

48 W. Liu, Y. Chen, H. Qi, L. Zhang, W. Yan, X. Liu, *et al.*, A Durable Nickel Single-Atom Catalyst for Hydrogenation Reactions and Cellulose Valorization under Harsh Conditions, *Angew. Chem., Int. Ed.*, 2018, **57**(24), 7071–7075.

49 X. Zhang, D. Wang, G. Wu, X. Wang, X. Jiang, S. Liu, *et al.*, One-pot template-free preparation of mesoporous MgO-ZrO_2 catalyst for the synthesis of dipropyl carbonate, *Appl. Catal., A*, 2018, **555**, 130–137.

50 X. Jiang, D. Savithri, X. Du, S. Pawar, H. Jameel, H. M. Chang and X. Zhou, Fractionation and characterization of kraft lignin by sequential precipitation with various organic solvents, *ACS Sustainable Chem. Eng.*, 2016, **5**(1), 835–842.